

Date of publication xxxx 00, 0000, date of current version xxxx 00, 0000.

Digital Object Identifier 10.1109/ACCESS.2017.Doi Number

# Enhanced Switching Pattern to Improve Cell Balancing Performance in Active Cell Balancing Circuit using Multi-winding Transformer

**Sang-Jung Lee<sup>1</sup>, Member, IEEE, Myoungcho Kim<sup>1</sup>, Member, IEEE, Ju-Won Baek<sup>1</sup>, Member, Dae-Wook Kang<sup>1</sup>, Member, IEEE, Jee-Hoon Jung<sup>2</sup>, Senior Member, IEEE**

<sup>1</sup>Korea Electrotechnology Research Institute (KERI), Power Conversion System Research Center, Changwon, 51543 South Korea

<sup>2</sup>Ulsan National Institute of Science and Technology (UNIST), School of Electrical and Computer Engineering, Ulsan, 44919 South Korea

Corresponding author: Jee-Hoon Jung (e-mail: jhjung@unist.ac.kr, jung.jeehoon@gmail.com).

This work was supported by Korea Electrotechnology Research Institute (KERI) Primary research program through the National Research Council of Science & Technology (NST) funded by the Ministry of Science and ICT (MSIT) (No. 20A01050).

**ABSTRACT** Cell balancing performance is an important factor in determining the operational efficiency of the active cell balancing circuit. Thus, this study approached this need by developing an enhanced switching pattern. The circuit is designed to transfer energy between arbitrary source and target cells. It has been operated in flyback and buck-boost modes according to the position of the source and target cells. In this circuit, the coupling coefficient of the transformer considerably affects the balancing performance of the flyback operation. The energy transferred to the non-target cell is increased by the low-coupling coefficient due to the leakage inductance. Therefore, the high energy transfer ratio cannot be achieved using conventional switching patterns. In this paper, a new flyback switching pattern is proposed, which can minimize the effect of the coupling coefficient in the cell balancing operation. The proposed switching pattern uses the cells which do not participate in the balancing process to control the voltage applied to each winding, which results in a high energy transfer ratio irrespective of the coupling coefficient. In addition, an enhanced operating method has been proposed to improve the cell balancing speed by reducing the energy transfer path in specific cell conditions. The performance of the proposed switching pattern was verified in a 15 W cell balancing circuit.

**INDEX TERMS** Battery management systems, Energy storage, Lithium-ion batteries, Flyback transformer

## I. INTRODUCTION

Recently, the paradigm of the automobile industry is changing due to greenhouse gas (GHG) emission restrictions and environmental regulations. The low-emission, high-efficiency, eco-friendly vehicle attracts attention, and the electric vehicle (EV) market is rapidly expanding. Power density is a significant factor in EV systems. Therefore, a lithium-ion battery (LIB) which has high energy and power density has been used as the main power source. Typically, a single cell of the LIB used in an EV battery system has low nominal voltage from 3.4 to 3.7 V. To smoothly supply power to the load, which requires high voltage, the lithium-ion batteries are used in a module form where the plurality of cells is connected in series. When multiple cells are connected in series, the same current flows through each cell. Therefore, if the initial state-of-charge (SoC) of each cell

connected in series is the same, the amount of energy stored in each cell should be the same after repeated charging and discharging.

In practice, however, the voltage difference between series-connected cells can occur from unbalance of the chemical characteristics and/or parameter changes inside the cells [1]. When cell voltage imbalance is present and the cells are repeatedly being charged and discharged, the voltage difference will grow worse and worse. In the worst case, a specific cell may be overcharged or over-discharged. This is a major cause of deterioration in cell lifetime and performance. To prevent the above problems, the battery management system (BMS) includes a cell balancing function, which is mainly composed of a software equalization strategy and a hardware cell balancing circuit. The equalization strategy is aimed at mitigating inter-cell

inconsistency, which can be largely classified into three strategies according to the equalization variables [2-4]. The first strategy is an operating voltage-based equalization, which equalizes the operating voltage of the cells. This strategy is simple and computationally efficient, but the accuracy of the operating voltage can be degraded by the cell internal parameters and external environments. The second strategy is a SoC-based equalization. This method can make the most of the cell power and avoid aging by over-discharge. However, it is relatively difficult to obtain accurate SoC estimation in a real-time manner while considering temperature and aging. Besides, the complex SoC estimation algorithm increases computational complexity and requires high-performance controllers. The last strategy is a capacity-based equalization strategy, which uses total capacity, rechargeable capacity, and releasable capacity as the equalization variables. This strategy maximizes the capacity utilization of the battery pack, but it has the disadvantages of difficulties in accurate capacity estimation and complex algorithms.

Based on the equalization strategy, the hardware cell balancing circuit performs cell equalization through the charging and discharging process. Until recently, various cell balancing techniques have been studied [5-10]. The cell balancing technology can be categorized into two types of methods: passive and active [11-14]. The passive method uses a resistor to dissipate the energy charged in a cell, which has relatively high voltage. This method has an advantage of the simple circuit configuration. However, whenever the cell voltage imbalance occurs, the energy charged in the cell is dissipated. This greatly reduces energy efficiency. Also, the heat generated by the resistors requires a cooling system. This greatly increases the size of the system.

In the active method, the cell voltage balancing is performed using energy storage elements such as capacitors and inductors [15-18]. The active method transfers the cell energy from a high voltage cell to a low voltage cell. There is no burn-out of the cell energy in the active method. Therefore, its energy efficiency is higher than that of the passive method, and as a result of higher balancing current, the cell balancing speed can be improved.

The active method can be further divided into three types. The first type is a module-to-cell method that uses the isolated dc/dc converter to transfer the energy stored in the module to a specific cell. This method has advantages of high efficiency and fast balancing speed. However, it has a complicated structure since the converter is connected to each cell. The second type is a cell-to-cell distributed method that transfers the energy between adjacent cells. Although direct energy transfer is possible between adjacent cells using this method, when the energy is transferred between non-adjacent cells, it requires multiple steps to transfer the energy to the target cell. These multiple transfer steps make efficiency and balancing speed worse. In addition, the balancing circuit requires a relatively large number of

passive components because the energy storage elements should be installed between every two adjacent cells. Finally, a cell-to-cell shared method can directly transfer the energy between adjacent and non-adjacent cells. It has a single energy storage element that can be shared by every cell so that a smaller number of passive elements is required. Also, the efficiency and balancing speed are better than those of the distributed method. However, the cell-to-cell shared method requires a complex switch structure to control the connection between the energy storage element and each cell. A balancing circuit proposed in [19] is affiliated to the cell-to-cell shared method and a multi-winding transformer is used as the energy storage element. Two semiconductor switches per each cell are required to control the connection between each cell and the multi-winding transformer. This structure makes the volume of the circuit increase significantly as the number of cells increases. To overcome this disadvantage in the previous study, a new cell balancing circuit using multi-winding transformers was proposed [20]. This balancing circuit has the same circuit structure and operation principle as [19] except that only one power semiconductor switch is required per cell. The circuit performs the cell balancing process using two operating modes: buck-boost and flyback. When transferring energy between adjacent cells that share a transformer winding, this circuit operates under the buck-boost mode. At this time, the transformer operates as a single inductor.

On the other hand, when transferring energy between odd- and even-numbered cells that do not share the identical transformer winding, this circuit operates under the flyback mode, and the transformer has the same energy transfer mechanism as a coupled inductor used in the conventional flyback converters. In practice, however, not all energy stored in the transformer is transferred to the target cell because parasitic components such as the transformer's leakage inductance and MOSFET's anti-parallel diodes create undesired current paths. The energy stored in the transformer is transferred to the non-target cell (the cell located at the bottom of the source cell) as well as the target cell by the undesired current paths. As the leakage inductance increases, the amount of energy delivered to the non-target cell increase. This phenomenon not only greatly reduces the cell balancing efficiency, but also causes a new cell imbalance during the balancing process. In this paper, the operational principles of the circuit and the cause of the undesired current path generated by the parasitic components are analyzed. After that, a new switching pattern is proposed to effectively transfer the balancing current to the target cell. Using the proposed switching pattern, it is possible to effectively transfer energy to the target cell even under conditions with a low coupling coefficient. As a result, precise energy transfer can be achieved, and the cell balancing circuit efficiency and the balancing speed are greatly improved. Besides, a new operation mode is proposed, which can significantly increase the balancing

speed under specific cell unbalance conditions. In the conventional circuit operation, when transferring energy between non-adjacent odd or even-numbered cells, the sequential operations of the buck-boost and flyback modes are required. Therefore, the number of the energy transfer path increases about 2 times more than those of other conditions, which spends more time in the balancing process. To compensate the above weakness, a forward operation mode is proposed. The proposed forward operation mode transfers energy between non-adjacent odd cells or even-numbered cells only during a single operation like the buck-boost mode or the flyback mode. As a result, the balancing speed can be drastically improved. The proposed switching and operating methods will be verified by the cell balancing experiments with a 15 W prototype cell balancing circuit.

## II. ANALYSIS OF CONVENTIONAL CELL BALANCING METHOD

In this section, the circuit operation of the conventional flyback operation will be analyzed by considering non-ideal parts of the circuit. To evaluate the switching method in terms of the energy transfer performance, the energy transfer ratio is defined as the ratio of the received energy at the target cell over the supplied energy from the source cell. Note that the definitions of the energy transfer ratio and the efficiency ( $\eta_e$ ) of the cell balancing circuit are different from each other. The operating mode analysis shows the influence of the coupling coefficient on the energy transfer ratio. In the conventional switching method, it is a good index to compare the balancing performance between the conventional and the proposed switching methods.

Before analyzing each operating mode, several assumptions are required as follows: First, this circuit can be applied to any number of the series-connected cells but multiple of two. In this paper, the balancing operation is explained by the circuit analysis with four series-connected cells, because it can cover every cases of the balancing operation. Second, the coupling of the multi-winding transformer is not perfect. The multi-winding transformer contains the leakage inductance. Third, each winding is assumed to have the same value of the leakage inductance. Finally, there is no cell voltage fluctuation during the switching cycle because the balancing current is small enough according to the power capacity of the cell. Fig. 1 (a), (b) and (c) show the current paths of mode 1, mode 3, and mode 4 in the conventional method, and Fig. 2 (a) shows the theoretical waveforms of each mode. The flyback operation can transfer the electric charge between the non-adjacent odd- and even-numbered cells. Note that the odd- and the even-numbered cells do not share the winding of the transformer. The analysis of the operating mode will be presented by assuming that the source cell and the target cell are cell 1 and cell 4, respectively.

Mode 1[ $t_0-t_1$ ]: Fig. 1 (a) shows the current path in mode 1.

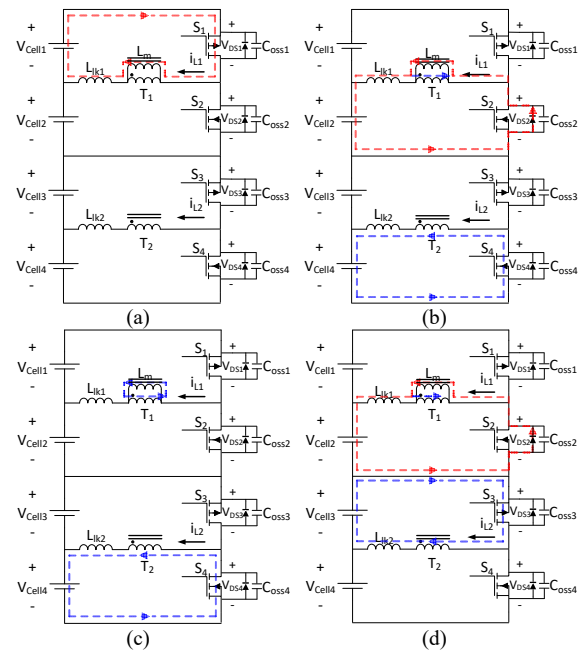


Fig. 1 Current path of cell balancing circuit in flyback operation: (a) ~ (c) Mode 1, 3, and 4 in the conventional method, (d) Mode 2 in the proposed method.

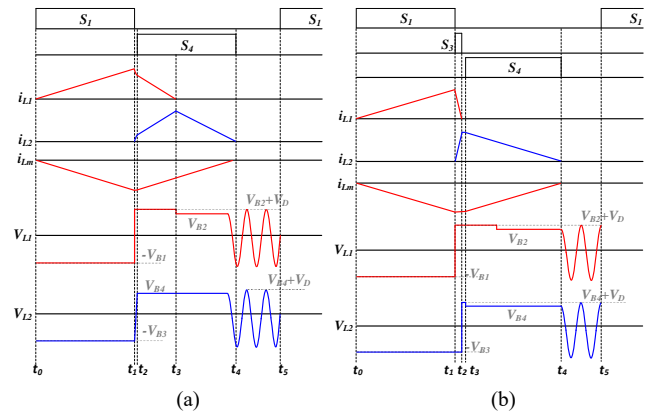


Fig. 2 Theoretical waveforms of the conventional flyback operation: (a) Conventional flyback operation, (b) Proposed flyback operation.

The switch  $S_1$  is turned on, and the energy stored in the cell 1 builds the magnetic energy in  $L_m$  and  $L_{lk1}$ . The slope of  $i_{L1}$  can be expressed as follows:

$$i_{L1}(t) = \frac{V_{cell1} - V_{ds}}{L_{lk} + L_m}(t - t_0) = \frac{V_{cell1}}{L_s}(t - t_0) \quad (1)$$

where  $V_{cell1}$  is the voltage of cell 1 and  $V_{ds}$  is the voltage applied to the MOSFET. The latter variable is negligible because it is minuscule compared with the cell voltage.

Mode 2[ $t_1-t_2$ ]: Before turning on  $S_4$ , dead-time between mode 1 and mode 3 is needed.

Mode 3[ $t_2-t_3$ ]: When  $S_4$  is turned on, the energy stored in  $L_m$  begins to transfer to the target cell through the current path of  $i_{L2}$ . In the ideal transformer model, when  $S_4$  turns on, the current  $i_{L1}$  decreases to zero by infinite negative slope,

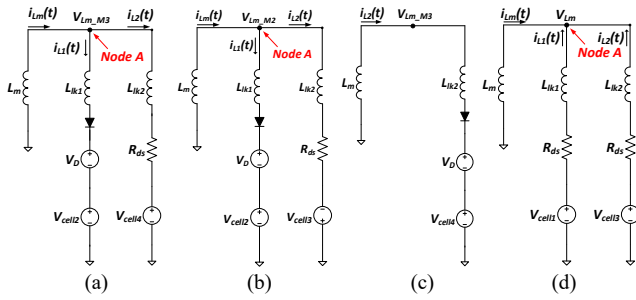


Fig. 3 Equivalent circuit diagram of the balancing circuit in flyback operation: (a) Mode 3 in the conventional method, (b), (c) Mode 2, 3 in the proposed method, (d)  $S_1$  and  $S_3$  are turned on simultaneously in the proposed method.

and all the energy stored in  $L_m$  is transferred to the target cell. However, in the practical transformer model, the current  $i_{L1}$  decreases by a constant slope due to the undesired current path caused by  $L_{lk}$  and  $D_2$ . The current  $i_{L1}$  and  $i_{L2}$  can be expressed as follows:

$$i_{L1}(t) = i_{L1,t2} + \left( \frac{V_{Lm,M3} - V_{Cell2} - V_D}{L_{lk1}} \right) (t - t_2) \quad (2)$$

$$i_{L2}(t) = i_{L2,t2} + \left( \frac{V_{Lm,M3} - V_{Cell4}}{L_{lk2}} \right) (t - t_2) \quad (3)$$

where  $V_{Lm,M3}$  is the average voltage applied to  $L_m$  in mode 3. Fig. 3 (a) shows the equivalent circuit of the multi-winding transformer in mode 3. The voltage of  $V_{Lm,M3}$  can be calculated by applying KCL to node A and can be expressed as shown in (4).

$$V_{Lm,M3} = \left( \frac{2V_{Cell} + V_D}{L_{lk} + 2L_m} \right) L_m \quad (4)$$

According to (2) and (3), the slopes of  $i_{L1}$  and  $i_{L2}$  are determined by the coupling coefficient. The low coupling coefficient decreases the current slope of  $i_{L1}$  and  $i_{L2}$  in mode 3. In addition, the direction of the slope of  $i_{L2}$  is determined by the magnitude of  $V_{Lm,M3}$ . If  $V_{Lm,M3}$  is smaller than  $V_{Cell4}$  due to the decrement of the coupling coefficient, the current slope of  $i_{L2}$  becomes negative. In this case, the current path of  $i_{L2}$  does not exist even if the switch  $S_4$  turns on because the multi-winding transformer operates as a single inductor. As a result, the energy stored in  $L_m$  is transferred to the non-target cells (cell 2) through the current path of  $i_{L1}$ . The duration of mode 3, the energy transferred to the non-target cell, can be calculated as shown in (5).

$$t_3 - t_2 = \left( \frac{L_{lk1}}{V_{Cell2} + V_D - V_{Lm,M3}} \right) i_{L1,t2} \quad (5)$$

Mode 4 [ $t_3-t_4$ ]: Mode 4 starts when  $i_{L1}$  reaches 0. In this mode, the current path can be represented as shown in Fig. 1 (c). All the energy stored in  $L_m$  is transferred to the target cell. The interval can be expressed as follows:

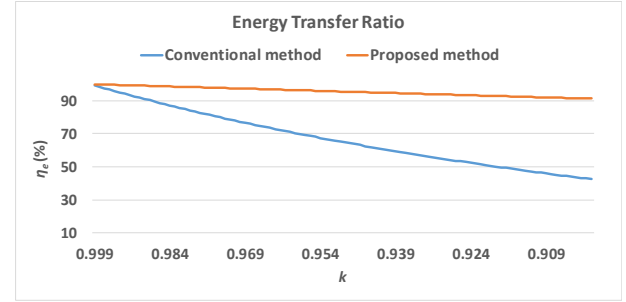


Fig. 4 Energy transfer ratio in flyback operation.

$$t_4 - t_3 = \frac{L_s}{V_{Cell4}} i_{L2,t3} \quad (6)$$

Mode 5 [ $t_4-t_5$ ]: During this mode, after all the energy stored in  $L_m$  is transferred to the target cell, the resonance between  $C_{oss}$  and  $L_s$  occurs until the next switching of  $S_1$ .

As a result of the analysis, the energy transferred to the non-target cell happens in mode 3 because the slopes of the current  $i_{L1}$  and  $i_{L2}$  are decreased by  $L_{lk}$ . Fig. 4 shows the effect of the coupling coefficient with the energy transfer ratio of the conventional flyback method and the proposed cell method. All the parameters used in the energy transfer ratio calculation are shown in Table I. Equations (7) and (8) show the amount of charge coming from the source cell and the amount of charge transferred to the non-target cell, respectively. The energy transfer ratio,  $\eta_e$ , is expressed as shown in (9).

$$q_{source} = \int_{t_0}^{t_1} i_{L1}(t) dt \quad (7)$$

$$q_{non\_target} = \int_{t_1}^{t_2} i_{L1}(t) dt \quad (8)$$

$$\eta_e = \frac{q_{source} - q_{non\_target}}{q_{source}} \quad (9)$$

In the conventional cell balancing method, the coupling coefficient has a great influence on the energy transfer ratio. As the coupling coefficient decreases, the energy transferred to the target cell decreases sharply. In order to improve the system efficiency, the coupling coefficient of the transformer should be close to unity. However, in practice, there is a limit to obtain a high coupling coefficient. There is leakage inductance in the transformer winding and there are many parasitic components that act as leakage inductance such as PCB trace, and the wire cable to connect between the battery and the balancing circuit. Therefore, the effect of the coupling coefficient should be minimized to improve the cell balancing performance.

### III. PROPOSED CELL BALANCING METHOD

#### A. Flyback operation

In the conventional cell balancing method, the energy transfer ratio is greatly affected by the coupling coefficient



of the transformer. In this subsection, a new cell balancing method for the flyback operation is proposed to minimize the energy transferred to the non-target cell by reducing the effect of the coupling coefficient. The proposed method controls the voltage applied to the transformer winding connected to the target cell using the switches of the non-target cell which shares the transformer winding with the target cell. Fig. 2 (b) shows the theoretical waveforms of each operating mode. Using Fig. 2 (b), the analysis of the mode operations will be presented by assuming that the source cell and the target cell is cell 1 and cell 4, respectively. The detailed analysis for each mode is as follows:

**Mode 1** [ $t_0-t_1$ ]: The switch  $S_1$  is turned on to build up the energy in  $L_m$ . The energy stored in cell 1 is transferred to  $L_m$  and  $L_{lk1}$ . The current  $i_{L1}$  in this period is the same as (1) shown in the analysis of mode 1 for the conventional flyback operation.

**Mode 2** [ $t_1-t_2$ ]: Fig. 1 (d) shows the current path in mode 2 of the proposed switching method. Unlike the conventional flyback operation, additional switching operations are required to reduce the energy delivered to the non-target cell. When  $S_3$  turns on, this mode starts. The direction of the current passing through each winding is the same as that of mode 3 of the conventional flyback operation. In the conventional method, the same voltage polarity is applied to each winding by the direction of the current passing through each winding. However, by turning on  $S_3$ , the voltage across cell 3 which has the opposite voltage polarity across  $L_1$  is forcibly applied to the winding of the cell 2. Fig. 3 (b) shows the equivalent circuit in mode 2. The interval of mode 2 can be calculated by (10), and  $V_{Lm,M2}$  can be expressed as (11) by applying KCL to node A.

$$t_2 - t_1 = \left( \frac{L_{lk1}}{V_D + V_{Cell2} - V_{Lm,M2}} \right) i_{L1,t1} \quad (10)$$

$$V_{Lm,M2} = \left( \frac{V_D}{L_{lk} + 2L_m} \right) L_m \quad (11)$$

The formula of the interval of mode 2 is the same as the interval of mode 3 in the conventional flyback operation. However,  $V_{Lm,M2}$  is smaller than  $V_{Lm,M3}$  in the conventional flyback operation. It is about two times smaller than the diode forward voltage drop, thereby increasing the voltage across  $L_{lk1}$ . As a result, it is possible to minimize the energy delivered to the non-target cell (cell 2) by increasing the current slope of  $i_{L1}$ . This means that the effect of the coupling coefficient of the transformer can be reduced by using the proposed cell balancing method. Since the energy transferred to the non-target cell can be minimized, the balancing speed of the cell voltage can be improved even with the existence of the leakage inductance. Fig. 4 presents the improved energy transfer ratio with the proposed flyback operation compared to the conventional method.

In the proposed flyback operation, the dead-time between mode 1 and mode 2 is not required. If  $S_1$  and  $S_3$  turn on simultaneously with the small overlap between the turn-on time of  $S_1$  and  $S_3$ , the voltages across cell 1 and cell 3 are applied to each winding. In this case, since the voltage across  $L_{lk1}$  and  $L_{lk2}$  comes from the voltage difference between  $V_{Lm}$  and the cell voltage corresponding to each switch, the changes of  $i_{L1}$  and  $i_{L2}$  are negligible. The voltage  $V_{Lm}$  can be expressed with the equivalent circuit shown in Fig. 3 (d) as follow:

$$V_{Lm} = \left( \frac{2V_{Cell}}{2L_m + L_{lk}} \right) L_m \cong V_{Cell} \quad (12)$$

**Mode 3** [ $t_2-t_3$ ]: Before  $S_4$  turns on, the dead-time is necessary to avoid shoot-through failure. Mode 3 also indicates the dead-time. The voltage  $V_{Lm,M3}$  can be expressed with the equivalent circuit shown in Fig. 3 (c) as follows:

$$V_{Lm,M3} = \frac{V_D + V_{Cell4}}{1 + \frac{L_{lk}}{L_m}} \cong V_D + V_{Cell4} \quad (13)$$

Since the voltage across  $L_{lk}$  is very small, the variations of  $i_{L1}$  and  $i_{L2}$  are negligible. The current equation of  $i_{L2}$  can be expressed as shown in (14)

$$i_{L2}(t) = \left( \frac{V_{Lm,M3} - V_D - V_{Cell4}}{L_{lk2}} \right) (t - t_2) \cong 0 \quad (14)$$

**Mode 4** [ $t_3-t_4$ ]: This mode starts when  $S_4$  turns on. In this mode, all the energy stored in  $L_m$  is transferred to the cell 4. The analysis of this interval is the same as mode 4 of the conventional flyback operation.

**Mode 5** [ $t_4-t_5$ ]: During this mode, after all the energy stored in  $L_m$  is transferred to the target cell, the resonance between  $C_{oss}$  and  $L_s$  occurs until the next switching period of  $S_1$ .

## B. Forward operation

In the conventional cell balancing method, both the buck-boost and flyback operations are used successively when the cell balancing is achieved between non-adjacent even-numbered or odd-numbered cells. Assuming that the source and the target cell is cell 1 and cell 3, respectively, the energy stored in the source cell can be transferred to the target cell by two steps. In the first step, the energy stored in the cell 1 is transferred to the cell 2 by the buck-boost operation. The buck-boost switching pattern is similar to that of the conventional flyback operation. The switch located in the source cell (cell 1) turns on to store the energy in the transformer, and the switch located in the cell 2 turns on to transfer the energy stored in the transformer to the cell 2. In the second step, the energy stored in the cell 2 is transferred to the cell 3 by the flyback operation. If the average balancing current of each operation is all the same, the

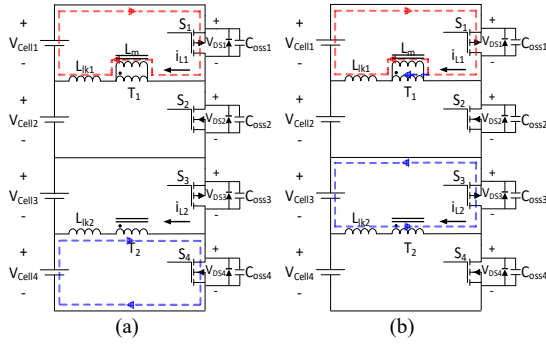


Fig. 5 Current paths of cell balancing circuit in the proposed forward operation: (a) Mode 1, (b) Mode 3.

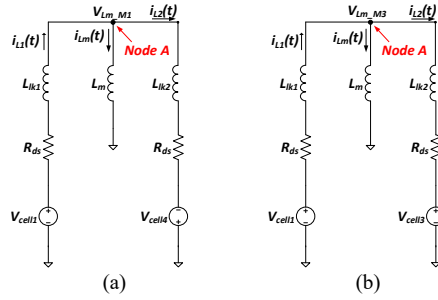


Fig. 6 Equivalent circuit diagram of cell balancing circuit in the proposed forward operation: (a) Mode 1, (b) Mode 3.

balancing speed is reduced to half of the single stage of the flyback or buck-boost operations. To avoid the above demerits, an enhanced cell balancing method is proposed in this paper. This operation can transfer the energy between non-adjacent even- or odd-numbered cells in a single operation like the flyback and the buck-boost operations without the balancing speed reduction. When the average balancing current is identical, the balancing speed can be improved around two times faster than that of the conventional method. The proposed method is named as the forward operation since the transformer delivers the cell energy to the other cell like a typical forward converter. Fig. 5 and 6 show the current path and the equivalent circuit corresponding to mode 1 and mode 3 of the proposed forward operation, respectively. They are used for the analysis of the current paths in each mode. The current path and equivalent circuit for other modes are omitted because they are repeated in the operating modes of the proposed flyback method. Fig. 7 shows the theoretical waveforms of each operating mode. The analysis includes the effect of the turn-on resistance of the MOSFETs since the effect of the turn-on resistance is more significant than the case of the flyback operation. From Fig. 7, the analysis of the mode operations will be presented. The detailed analysis for each mode is as follows:

**Mode 1** $[t_0-t_1]$ : When  $S_1$  and  $S_4$  turn on simultaneously, mode 1 starts. In this mode, the current  $i_{L2}$  which has a direction to charge the target cell is generated. When both the switches turn on simultaneously, since alternative voltage polarities are applied to each winding, the voltages

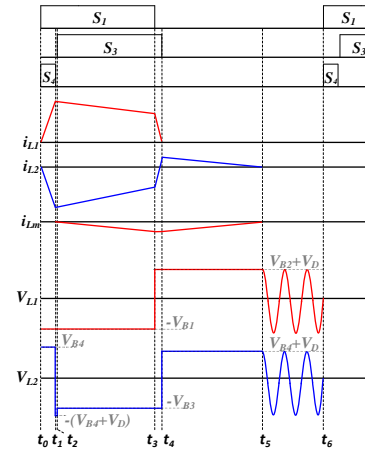


Fig. 7 Theoretical waveforms of the proposed forward operation.

of the cells corresponding to the switches are applied to  $L_{lk1}$  and  $L_{lk2}$ . Thus, the energy is not stored in  $L_m$  but only the currents of  $i_{L1}$  and  $i_{L2}$  are generated. Fig. 6 (a) shows the equivalent circuit during mode 1, and the current equations of  $i_{L1}$  and  $i_{L2}$  can be expressed as shown in (15).

$$i_{L1}(t) = i_{L2}(t) = \frac{V_{cell}}{R_{ds}} \left( 1 - e^{-\frac{R_{ds}t}{L_{lk}}} \right) \quad (15)$$

The peak magnitude of the current is determined by the required average value of the balancing current. When the peak value of the current is chosen, the duration of mode 1 can be determined by  $R_{ds}$  and  $L_{lk}$ . As the two parasitic components increase, the duration of mode 1 becomes longer, and more energy is discharged from cell 4 to generate the peak magnitude of the current. If the discharged energy of cell 4 is not compensated, a new cell imbalance may occur due to the decrement of  $V_{cell4}$  during the balancing process. Therefore, it is necessary to compensate for the energy discharged from cell 4.

**Mode 2** $[t_1-t_2]$ : When  $S_4$  turns off, mode 2 starts. The dead-time duration is required to prevent shoot-through faults before  $S_3$  turns on. In this interval, only  $S_1$  turns on. During the dead-time interval,  $i_{L2}$  completely discharges and charges  $C_{oss3}$  and  $C_{oss4}$ ; then it flows through the antiparallel diode of  $S_3$ .

**Mode 3** $[t_2-t_3]$ : When  $S_3$  turns on, mode 3 starts. The energy discharged from the source cell begins to transfer to the target cell through the transformer and charge  $L_m$  at the same time. In this mode, the current equation of  $i_{L1}$ ,  $i_{L2}$  and  $i_{Lm}$  can be expressed with the equivalent circuit shown in Fig. 6 (b) as follows:

$$i_{L1}(t) = \frac{V_{cell} - V_{Lm}(t)}{R_{ds}} \left( 1 - e^{-\frac{R_{ds}t}{L_{lk}}} \right) + i_{L1,t2} e^{-\frac{R_{ds}t}{L_{lk}}} \quad (16)$$

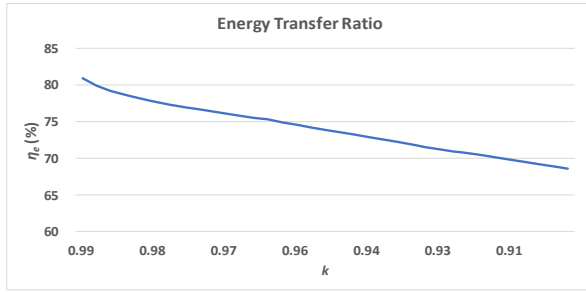


Fig. 8 Energy transfer ratio in the proposed forward operation according to the coupling coefficient.

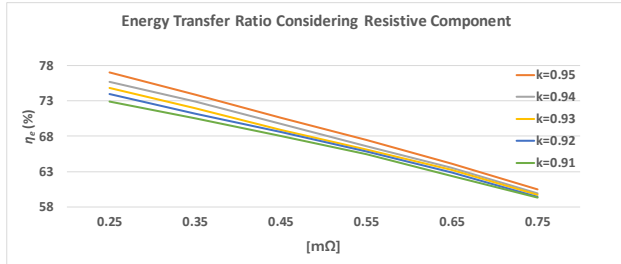


Fig. 9 Energy transfer ratio in the proposed forward operation considering different resistance component.

$$i_{L2}(t) = \frac{V_{Lm}(t) - V_{Cell}}{R_{ds}} \left( 1 - e^{-\frac{R_{ds}t}{L_{lk}}} \right) + i_{L2,t2} e^{-\frac{R_{ds}t}{L_{lk}}} \quad (17)$$

$$i_{Lm}(t) = \frac{\left( \frac{2V_{Cell}}{R_{ds}} + \frac{2L_m i_{Lm,t2}}{R_{ds}t} \right)}{\left( \frac{1}{1 - e^{-\frac{R_{ds}t}{L_{lk}}}} \right) + \left( \frac{2L_m}{R_{ds}t} \right)} \quad (18)$$

If the MOSFET is an ideal model, the slope of  $i_{L1}$  and  $i_{L2}$  is determined by only  $L_{lk}$ , since  $R_{ds}$  is zero in the turn-on state. In practice, however, the MOSFET has several tens to hundreds of milli-ohm as the turn-on resistance, which increases the slope of the current  $i_{L1}$  and  $i_{L2}$  due to the decrement in the time constant. As a result, high turn-on resistance reduces the interval of mode 3. Therefore, it is advantageous to use the MOSFET which has low  $R_{ds}$  to achieve high energy transfer capability.

As mentioned earlier, it is necessary to compensate for the energy discharged from cell 4 during mode 1 to prevent the cell imbalance. To achieve the compensation, the energy stored in  $L_m$  during mode 3 is used. Therefore, this energy should be equal to the amount of energy discharged from cell 4 during mode 1.

**Mode 4 [ $t_3-t_4$ ]:** When  $S_1$  turns off, mode 4 starts. For the energy stored in  $L_m$  to be transferred to cell 4 in the energy compensation duration (next mode) of cell 4,  $S_3$  should be turned on until  $i_{L1}$  decreases to zero. If the current  $i_{L1}$  is not reduced to zero in mode 4, the current  $i_{L1}$  decreases with a constant slope by  $L_{lk}$  in the next mode due to the same phenomenon as mode 3 of the conventional flyback operation. This can cause cell imbalance phenomenon by transferring the energy stored in  $L_m$  to the non-target cell (cell

TABLE I. Design Parameters of Prototype Cell Balancing Circuit

| Parameters        |                            | Values        |
|-------------------|----------------------------|---------------|
| Balancing Circuit | $f_{sw}$                   | 50 [kHz]      |
|                   | $L_s$                      | 2.78 [μH]     |
|                   | $K$                        | 0.948 / 0.92  |
|                   | Turn ratio                 | 1:1           |
| Battery           | Model                      | SLPB120255255 |
|                   | Nominal voltage            | 3.7 [V]       |
|                   | Capacity                   | 75 [Ah]       |
| MOSFET            | $R_{DS,P-type}$ (SISS27DN) | 13 [mΩ]       |
|                   | $R_{DS,N-type}$ (SIR158DP) | 2.25 [mΩ]     |

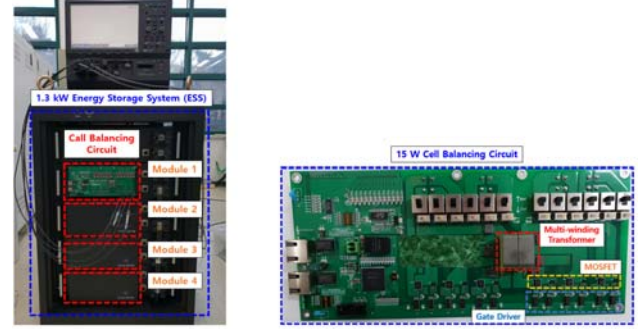


Fig. 10 12-cell series connected 15 W prototype cell balancing circuit.

2) located at the bottom of the source cell as well as cell 4. The equivalent circuit in mode 4 is the same as Fig. 1 (d), and the turn-on time of  $S_3$  can be expressed as follows:

$$t_4 - t_3 = \frac{\ln \left( -\frac{R_{ds} L_m i_{Lm,t3} + \alpha}{R_{ds} L_m i_{L2,t3} + \alpha} \right) (2L_m + L_{lk}) L_{lk}}{R_{ds} (L_m + L_{lk})} \quad (19)$$

$$\text{where } \alpha = (2L_m + L_{lk})V_{cell} + V_D L_m$$

**Mode 5 [ $t_4-t_5$ ]:** When  $S_3$  turns off, mode 5 starts. In this interval, the energy stored in  $L_m$  is transferred to cell 4. To compensate for the energy discharged in cell 4 during mode 1 and to prevent the core saturation of the transformer, the energy charged in  $L_m$  should be completely discharged before the next switching cycle. In mode 5, the equivalent circuit is the same as Fig. 3 (c), and the discharging time can be expressed as (20).

$$t_5 - t_4 = \frac{L_s}{V_{Cell4} + V_D} i_{L2,t4} \quad (20)$$

**Mode 6 [ $t_5-t_6$ ]:** After all the energy stored in  $L_m$  is discharged, the resonance with  $C_{oss}$  and  $L_s$  happens until the next switching period.

In the proposed forward operation, the energy stored in the source cell is discharged from mode 1 to mode 3, and the discharged energy is transferred to the target cell during mode 2 and mode 3. Therefore, the energy transfer ratio is affected by the duration of mode 1 and mode 4 in which the energy discharged from the source cell is not transferred to the target cell. Particularly, it is mainly determined by the duration of mode 1. The lower the coupling coefficient, the

smaller the current slope of  $i_{L1}$  and  $i_{L2}$ . Therefore, the duration of mode 1 increases and the energy transfer ratio decreases. However, the energy transfer ratio of the proposed balancing method is not significantly affected by the coupling coefficient comparing with that of the conventional flyback operation. Fig. 8 shows the energy transfer ratio in the proposed forward operation. The parameters used in the calculation of the energy transfer ratio are shown in Table I, and  $R_{ds}$  was assumed to 30 mΩ. As mentioned previously, the resistive component does not significantly affect the energy transfer ratio of the flyback and buck-boost operations. However, the energy transfer ratio of the forward operation is affected by the resistance due to the time constant presented in the current formula of each mode. Fig. 9 shows the effect of the resistive component ( $R_{ds}$ ) in the energy transfer ratio. The energy transfer ratio can be reduced not only by the low coupling coefficient, but also by the high resistive component. Therefore, minimizing the resistive component is advantageous for the energy transfer capability and energy transfer ratio of the forward operation.

#### IV. EXPERIMENTAL RESULTS

The analysis of the conventional and proposed switching patterns are verified by a 12-cell series connected 15 W cell balancing circuit shown in Fig. 10. Table I shows the design parameters of the cell balancing circuit. In the flyback, buck-boost and forward operations, the RMS current flowing through the transformer is assumed to be 4 A, and the multi-winding transformers with coupling coefficients of about 0.948 and 0.92 were used in the experiments. Since the low resistive component is essential for the forward operation, MOSFET with low  $R_{ds}$  are selected.

Fig. 11 (a) shows the switching signals and the transformer winding currents of the conventional flyback operation when the coupling coefficient is 0.948. After  $S_1$  turns off, a part of the energy stored in  $L_m$  by the leakage inductance is transferred to cell 2 until  $i_{L1}$  decreases to zero. In this case, the energy transfer ratio is around 68%. Fig. 11 (b) shows the switching signals and the transformer winding currents of the proposed operation. The amount of energy delivered to cell 2 is reduced by turning on  $S_3$  before  $S_4$  turns on. By using the proposed cell balancing method, most of the energy stored in  $L_m$  can be effectively transferred to cell 4. In this case, the energy transfer ratio is around 96%. The energy transfer ratio improved by the proposed system around 28% compared with the conventional cell balancing method.

Fig. 12 shows the winding current waveforms in the flyback operation when the coupling coefficient is 0.92. In the conventional switching method, the energy transfer ratio is about 50%. As the coupling coefficient decreases, the energy transferred to the non-target cell increases significantly. However, when the proposed switching method is used, the energy transfer ratio of 92% can be achieved. The experiments have shown that the proposed switching method can significantly improve the energy

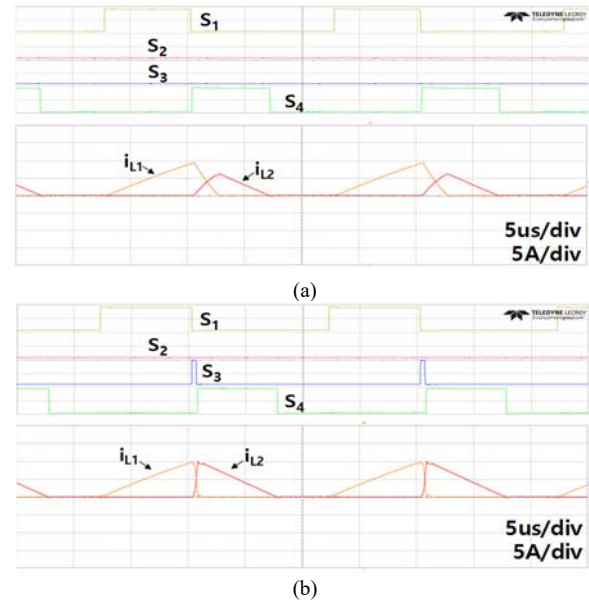


Fig. 11 Experimental waveforms ( $k=0.948$ ) : (a) Switching signals and current waveforms in the conventional flyback operation (5us/div) (b) Switching signals and current waveforms in the proposed flyback operation (5us/div).

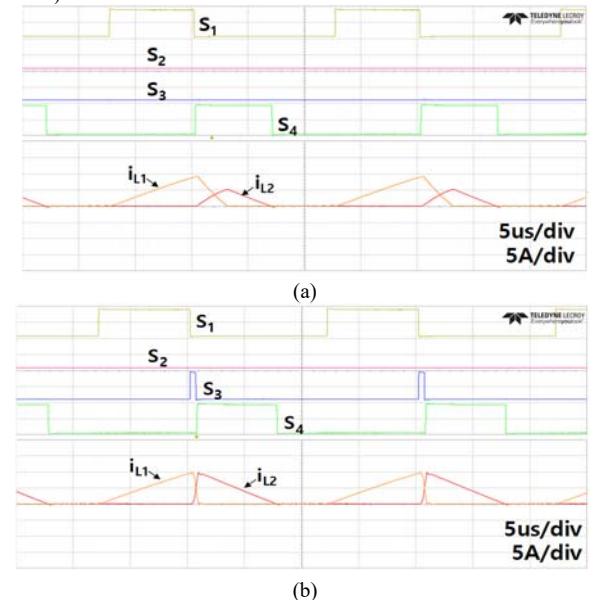


Fig. 12 Experimental waveforms ( $k=0.92$ ) : (a) Switching signals and current waveforms in the conventional flyback operation (5us/div) (b) Switching signals and current waveforms in the proposed flyback operation (5us/div).

transfer ratio even with low coupling coefficients. Fig. 13 (a) shows the switching signals and the transformer winding currents of conventional buck-boost operation when the coupling coefficient is about 0.948. Even using the conventional cell balancing method, the energy stored in the source cell (cell 1) can be effectively transferred to the target cell (cell 2). In this case, the energy transfer ratio can approach 99%. The experimental results show that the leakage inductance does not affect the energy transfer ratio of the buck-boost operation. Fig. 13 (b) shows the switching signals and the transformer winding currents of the proposed



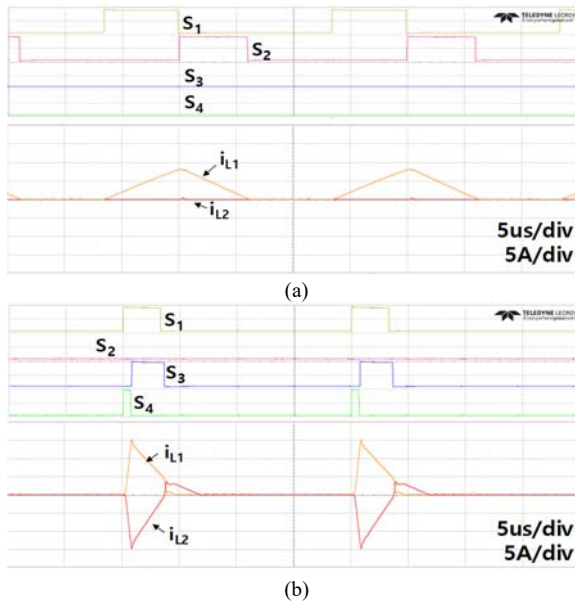


Fig. 13 Experimental waveforms ( $k=0.948$ ) : (a) Switching signals and current waveforms in the conventional buck-boost operation (5us/div), (b) Switching signals and current waveforms in the proposed forward operation (5us/div).

forward operation. Using the proposed cell balancing method, the energy stored in cell 1 can be transferred to cell 3 in a single switching cycle. By shortening the energy transfer path, the balancing speed can be improved. However, the current slope in the duration when the energy is transferred to the target cell is increased by the MOSFET's  $R_{ds}$ . Also, the average current of the forward operation is smaller than that of the flyback operation even under the same RMS current condition.

To compare the balancing speed between using the conventional and proposed switching patterns, the cell balancing experiment is achieved by using the 15 W cell balancing circuit. Cell balancing was performed using operating voltage-based equalization strategies considering overpotential according to the balancing current. Table II shows the initial voltage and the SoC of each cell before the balancing operation. Table III shows the balanced voltage and the SoC of each cell after the balancing operations. The SoC was estimated based on the OCV-SoC relationship acquired with a cell charging/discharging test. The OCV during the cell balancing operation is estimated with the overpotential of cell. The overpotential of the cell is experimentally measured for the designed balancing current, 4Arms. The results are summarized in Table III. Under all the balancing operations, the initial voltage difference between the source and target cells becomes around 50 mV, and the SoC deviation comes to around 7.4%. For accurate voltage measurements, each cell voltage has been measured using a digital voltage sensor of LTC6804-2 manufactured by Analog Devices. It represents the cell voltage in a 16-bit resolution and has a precision of about 100  $\mu$ V. Fig. 14 (a) shows cell voltage waveforms using the conventional

TABLE IV. Comparison of Cell Balancing Performance

| Balancing conditions                      | $k : 0.948$          | Energy Transfer Ratio [%] | Balancing time [min] | Additional balancing operation |
|---|----------------------|---------------------------|----------------------|--------------------------------|
| Between non-adjacent odd and even # cells | Conventional Flyback | 68                        | 58                   | Required                       |
|   | Proposed Flyback     | 96                        | 45                   | Not required                   |
| Between non-adjacent odd # cells          | Buck-boost & Flyback | 96                        | 111                  | Not required                   |
|   | Proposed Forward     | 73                        | 56                   | Not required                   |

flyback operation. It takes about 58 minutes to equalize the voltage between cell 1 (source cell) and cell 4 (target cell). The voltage of cell 2 (non-target cell) increases by about 4.2 mV, and the SoC increases by about 0.6% during the cell balancing operation. The increment of the voltage across the non-target cell can cause an alternative cell imbalance. Therefore, when the flyback operation achieves during the cell balancing process, additional cell balancing operations can be required due to the leakage energy transferred to the non-target cell. This undesirable energy transfer decreases the cell balancing speed and the efficiency of the balancing circuit.

Fig. 14 (b) shows cell voltage waveforms using the proposed flyback operation. It takes approximately 45 minutes for the cell voltage balancing, which is 13 minutes shorter than the conventional method and improves the balancing speed around 1.3 times faster than that of the conventional method. Besides, the voltage change of cell 2 (non-target cell) is 0.2 mV during the balancing process, which is much less than that of the conventional method. Since additional cell balancing operations are not needed, the efficiency of the cell balancing operation can be improved. Fig. 14 (c) shows cell voltage waveforms in the conventional buck-boost operation. The source cell and the target cell are cell 1 and cell 2, respectively. The balancing time is approximately 1 hour and 6 minutes. When the cell balancing is achieved between cell 1 (source cell) and cell 3 (target cell) in the conventional cell balancing method, the balancing time is the sum of the flyback and buck-boost operations. This is because both the buck-boost and flyback operations must be used consecutively to transfer energy to the target cell. Therefore, the total balancing time of the conventional balancing method can be expected to be around 1 hour and 51 minutes. Fig. 14 (d) shows cell voltage waveforms in the proposed forward operation, and the balancing time is around 56 minutes. Compared with the conventional method, the balancing speed is 2 times faster. In addition, cell 2 and cell 4 which are non-target cells have only the little voltage variations of 0.6 mV and 2.1 mV, respectively, during the balancing process. Table IV shows the comparison of the cell balancing performance between the conventional method and the proposed method. From the experimental results, it can be verified that the proposed flyback switching pattern

and the forward operation mode can greatly improve the balancing speed.

## V. CONCLUSION

In this paper, the operation of the balancing circuit using the multi-winding transformer is theoretically analyzed. Also, the coupling coefficient effect of the transformer and antiparallel diode of the MOSFETs for the energy transfer ratio is analyzed. The conventional flyback operation is strongly affected by the coupling coefficient. Low coupling coefficient reduces the energy transfer ratio by creating a path that transfers the cell energy to the non-target cells. This additional path increases cell balancing time and causes cell imbalance during the balancing process, which reduces system efficiency. However, by using the proposed switching modulation method, it is possible to minimize the influence of the coupling coefficient in the flyback operation.

This paper also proposes the novel switching pattern which can transfer the cell energy to the target cell in a single operation. Experimental results show that the proposed switching pattern can improve the balancing speed by reducing the current path. The improvement of the proposed switching pattern is verified by the cell balancing experiments. By using the proposed switching method in the flyback operation with a coupling coefficient of 0.948, the energy transfer ratio is increased by a factor of 1.4, and the balancing speed is 1.3 times faster than the conventional switching method. Furthermore, when the balancing is performed by the proposed forward operation, the balancing speed is about 2 times faster than the conventional balancing method. The performance of the proposed switching scheme is verified by a 15 W cell balancing circuit.

TABLE II. Cell voltage and SoC measurements in the initial state

| Cell number | Conventional flyback |         | Proposed flyback    |         | Buck-boost          |         | Proposed forward    |         |
|-------------|----------------------|---------|---------------------|---------|---------------------|---------|---------------------|---------|
|             | Initial Voltage [V]  | SoC [%] | Initial voltage [V] | SoC [%] | Initial Voltage [V] | SoC [%] | Initial Voltage [V] | SoC [%] |
| Cell 1      | 3.5750               | 25.8    | 3.5755              | 25.89   | 3.5750              | 25.8    | 3.5755              | 25.9    |
| Cell 2      | 3.5498               | 21.83   | 3.5503              | 21.91   | 3.5245              | 18.33   | 3.5474              | 21.48   |
| Cell 3      | 3.5489               | 21.7    | 3.5493              | 21.76   | 3.5468              | 21.4    | 3.5259              | 18.51   |
| Cell 4      | 3.5250               | 18.39   | 3.5258              | 18.5    | 3.5465              | 21.35   | 3.5486              | 21.66   |

TABLE III. Cell voltage SoC measurements in the balanced state

| Cell number | Conventional flyback |         | Proposed flyback     |         | Buck-boost           |         | Proposed forward     |         |
|-------------|----------------------|---------|----------------------|---------|----------------------|---------|----------------------|---------|
|             | Balanced Voltage [V] | SoC [%] | Balanced voltage [V] | SoC [%] | Balanced Voltage [V] | SoC [%] | Balanced Voltage [V] | SoC [%] |
| Cell 1      | 3.5440               | 21      | 3.5474               | 21.48   | 3.5477               | 21.53   | 3.5449               | 21.12   |
| Cell 2      | 3.5540               | 22.46   | 3.5505               | 21.94   | 3.5474               | 21.48   | 3.5480               | 21.57   |
| Cell 3      | 3.5484               | 21.63   | 3.5484               | 21.63   | 3.5465               | 21.35   | 3.5458               | 21.24   |
| Cell 4      | 3.5443               | 21.03   | 3.5477               | 21.53   | 3.5461               | 21.29   | 3.5465               | 21.35   |

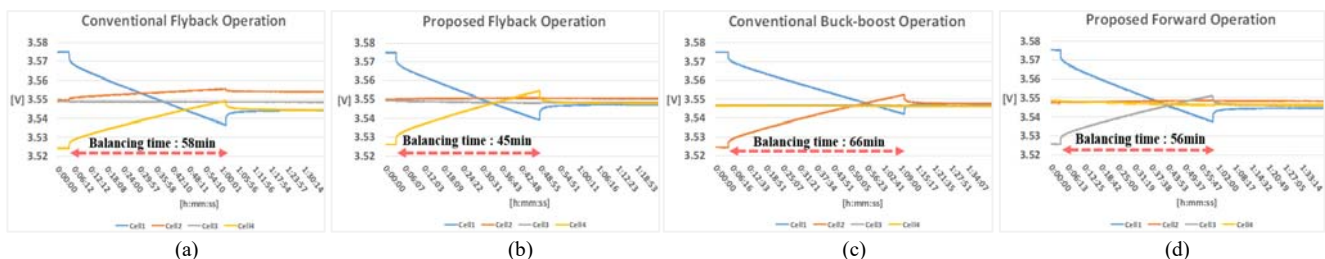


Fig. 14 Balancing speed of cell voltage according to operational methods: (a) Conventional flyback operation, (b) Proposed flyback operation, (c) Conventional buck-boost operation, (d) Proposed forward operation.

## VI. REFERENCE

- [1] J.-H Kim, J.-W Shin, C.-Y Chun, and B.-H. Cho, "Stable Configuration of a Li-Ion Series Battery Pack Based on a Screening Process for Improved Voltage/SOC Balancing", *IEEE Trans. Power Electronics*, vol. 27, pp. 411-424, Jan 2012.
- [2] F. Fei, H. Xiaosong, L. Jianfei, L. Xianke, L. Bo, "A review of equalization strategies for series battery packs: variables, objectives, and algorithms," *Renewable and Sustainable Energy Reviews*, Volume 116, pp. 109464, Dec. 2019.
- [3] F. Fei, H. Xiaosong, H. Lin, H. Fengling, L. Yang, Z. Lei, "Propagation mechanisms and diagnosis of parameter inconsistency within Li-Ion battery

packs," *Renewable and Sustainable Energy Reviews*, Volume 112, pp. 102-113, Sep. 2019.

- [4] F. Fei, L. Rengui and Z. Chunbo, "Equalisation strategy for serially connected LiFePO<sub>4</sub> battery cells," in *IET Electrical Systems in Transportation*, vol. 6, no. 4, pp. 246-252, 12 2016.
- [5] J. Qi and D. Dah-Chuan Lu, "Review of battery cell balancing techniques," *2014 Australasian Universities Power Engineering Conference (AUPEC)*, Perth, WA, 2014, pp. 1-6.
- [6] J. Cao, N. Schofield, and A. Emadi, "Battery balancing methods: A comprehensive review," in *Proc. IEEE Veh. Power Propulsion Conf.*, Sep. 2008, pp. 1-6.
- [7] Y.-S Lee and M.-W Cheng, "Intelligent control battery equalization for series connected lithium-ion battery strings," *IEEE Trans. Industrial Electronics*, vol. 52, pp. 1297-1307, Oct 2015.

- [8] Y.-S. Lee and G.-T. Cheng, "Quasi-resonant zero-current-switching bidirectional converter for battery equalization applications," *IEEE Trans. Power Electronics*, vol. 21, pp. 1213-1224, Sept 2006.
- [9] L.A. Tolbert, F.Z. Peng, T. Cunningham and J.N. Chiasson, "Charge balance control schemes for cascade multilevel converter in hybrid electric vehicles," *IEEE Trans. Industrial Electronics*, vol. 49, pp. 1058-1064, Oct 2002.
- [10] H.-S. Park, C.-E. Kim, C.-H. Kim, G.-W. Moon, and J.-H. Lee, "A modularized charge equalizer for an HEV lithium-ion battery string," *IEEE Trans. Power Electronics*, vol. 56, pp. 1464-1476, May 2009.
- [11] A. Baughman and M. Ferdowsi, "Double-tiered switched-capacitor battery charge equalization technique," *IEEE Trans. Industrial Electronics*, vol. 55, no. 6, pp. 2277-2285, Jun. 2008.
- [12] H.-S. Park, C.-E. Kim, C.-H. Kim, G.-W. Moon, and J.-H. Lee, "A modularized charge equalizer for an HEV lithium-ion battery string," *IEEE Trans. Industrial Electronics*, vol. 56, no. 5, pp. 1464-1476, May 2009.
- [13] S. Bergvik, "Prolonged Useful Life and Reduced Maintenance of Lead-acid Batteries by Mean of individual Cell Voltage Regulation," in *Proc. INTELEC Conf.*, 1984, pp. 63-66.
- [14] D. Bjork, "Maintenance of Batteries-new trend in batteries and automatic battery charging," in *Proc. INTELEC Conf.*, 1986, pp. 355-360.
- [15] N. H. Kutkut, "A modular nondissipative current divider for EV battery charge equalization," in *Proc. IEEE Appl. Power Electron. Conf.*, 1998, vol. 2, pp. 686-690.
- [16] C. Pascual and P. T. Krein, "Switched capacitor system for automatic series battery equalization," in *Proc. IEEE 1997 Applied Power Electronics Conf.*, pp. 848-854, 1997, Feb.
- [17] J.W. Kimball and P. T. Krein, "Analysis and design of switched capacitor converters," in *Proc. Appl. Power Electron. Conf. Expo.*, Mar. 2005, vol. 3, pp. 1473-1477.
- [18] X. Wei and B. Zhu, "The research of vehicle power Li-ion battery pack balancing method," in *Proc. IEEE 9th Int. Electron. Meas. Instruments Conf.*, Beijing, China, Aug. 2009, pp. 498-502.
- [19] S.-H. Park, K.-B. Park, H.-S. Kim, G.-W. Moon, and M.-J. Youn, "Single-Magnetic Cell-to-Cell Charge Equalization Converter With Reduced Number of Transformer Windings," *IEEE Trans. Power Electronics*, vol. 27, pp. 2900-2911, June 2012.
- [20] J. Xu, S. Li, C. M. Z. Chen and B. Cao, "SOC Based Battery Cell Balancing with a Novel Topology and Reduced Component Count," *Energies*, vol. 6, pp. 2726-2740, May 2013.



**Sangjung Lee** was born in Andong, South Korea, in 1990. He received the B.S. degree in electrical engineering from Kumoh National Institute of Technology, Gumi, South Korea, in 2015. He is currently working toward the combined Masters-PhD degree at Ulsan National Institute of Science and Technology (UNIST), Ulsan, South Korea. His research interests are Battery Management System and Hardware in-the-Loop (HIL) simulation for power management system function testing. Recently, he has been researching HVDC/MVDC, MTDC, and the applications of power electronics based on multilevel converter.



**Myoungcho Kim** received the B.S. degree in electrical engineering from Hanyang University, Seoul, in 2006 and the M.S. and Ph.D. degrees in electrical engineering from Seoul National University, Seoul, in 2008 and 2013, respectively. From 2013 to 2015, was a Manager at the Power and Control

Systems Division, Samsung Heavy Industries, Korea. Since 2016, he has been a Senior Researcher in Korea Electrotechnology Research Institute (KERI), Korea. His current research interests include circuit topology and controller design for various power converters.



**Ju-Won Baek** received the M.S. and Ph.D. degrees from Kyungpook National University, Taegu, Korea, in 1993 and 2002, respectively. Since 1993, he has been working as a Principle Researcher in smart grid division, Korean Electrotechnology Research Institute (KERI), Changwon, Korea. His primary research areas include soft-switching converters, power quality, high-voltage power supplies, power converter for renewable energy. Recently, he has been interested in dc distribution system and solid state transformer. Dr. Baek is a member of the Korean Institute of Power Electronics and the IEEE.



**Dae-Wook Kang** received the B.S., M.S., and Ph.D. degrees in electrical engineering from Hanyang University, Seoul, Korea, in 1998, 2000, and 2004, respectively. Since 2004, he had joined the Korea Electrotechnology Research Institute (KERI), Changwon, Korea. His present interests include HVDC/MVDC, MTDC, ESS, renewable energy, and the applications of power electronics based on multilevel converter.



**Jee-Hoon Jung** was born in Suwon, South Korea, in 1977. He received B.S. degree in the Electronic and Electrical Engineering and M.S. and Ph.D. degrees in the Electrical and Computer Engineering from Pohang University of Science and Technology (POSTECH), Pohang, South Korea, in 2000, 2002, and 2006, respectively. From 2006 to 2009, he was a Senior Research Engineer in the Digital Printing Division, Samsung Electronics Co. Ltd., Suwon, South Korea. From 2009 to 2010, he was a Postdoctoral Research Associate in the Electrical and Computer Engineering, Texas A&M University at Qatar (TAMUQ), Doha, Qatar. From 2011 to 2012, he was a Senior Researcher in the Power Conversion and Control Research Center, HVDC Research Division, Korea Electrotechnology Research Institute (KERI), Changwon, South Korea. From 2013 to 2016, he was an Assistant Professor in the School of Electrical and Computer Engineering, Ulsan National Institute of Science and Technology (UNIST), Ulsan, South Korea, where he is presently working as an Associate Professor. His research interests include DC-DC and AC-DC converters, switched-mode power supplies, digital control and signal processing algorithms, power conversion for renewable energy, and

real-time and power Hardware-in-the-Loop (HIL) simulations electric and industrial applications. Recently, he has been researching high-frequency power converters using wide bandgap devices, bidirectional power converters for smart grids, resonant power converters for induction heating (IH) systems, spread spectrum techniques for electromagnetic (EM) noise reduction, power line communications for DC microgrids, and wireless power transfer techniques for home appliances.

Dr. Jung is a Senior Member of the IEEE Industrial Electronics Society, the IEEE Power Electronics Society, the IEEE Industry Applications Society, and the IEEE Power and Energy Society. He had served as a Member of the Editorial Committee of the Korea Institute of Power Electronics (KIPE). He is presently serving as a Member of Board of Directors of the KIPE. In addition, he is an Associate Editor of the Journal of Power Electronics (JPE) and an Editorial Board Member of Energies in the Multidisciplinary Digital Publishing Institute (MDPI).